Electronic Supporting Information (ESI)

In-depth structural characterization of the influence of Li⁺ excess on spherical, Co-free layered LiMn$_{0.5}$Ni$_{0.5}$O$_2$ cathode material using correlative Raman-SEM microscopy

Florian Klein,[a] Claudia Pfeifer,[a] Philipp Scheitenberger,[b] Lukas Pfeiffer,[a] Dominik Zimmer,[c] Margret Wohlfahrt-Mehrens,[a] Mika Lindén*[,b] and Peter Axmann*[,a]

[a]Zentrum für Sonnenenergie- und Wasserstoffforschung Baden-Württemberg (ZSW),
Helmholtzstrasse 8, D-89081 Ulm (Germany).
e-mail: peter.axmann@zsw-bw.de

[b]Institute for Inorganic Chemistry II, Ulm University,
Albert-Einstein-Allee 11, D-89081 Ulm (Germany).
e-mail: mika.linden@zsw-bw.de

[c]Oxford Instruments GmbH,
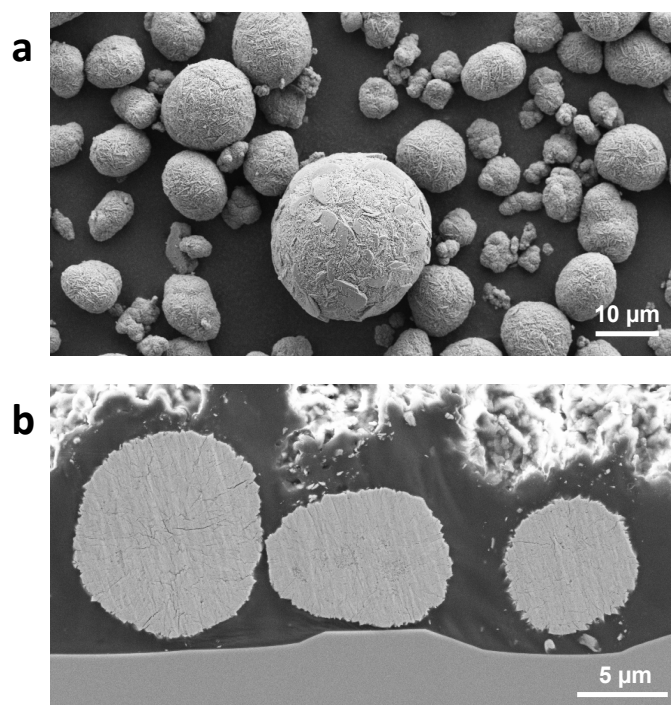Borsigstr. 15A, 65205 Wiesbaden (Germany)

Figure S1. SEM images of the (Mn$_{0.5}$Ni$_{0.5}$)(OH)$_2$ precursor: a) top view of spherical particle morphology and b) particle cross-section of dense spheres.
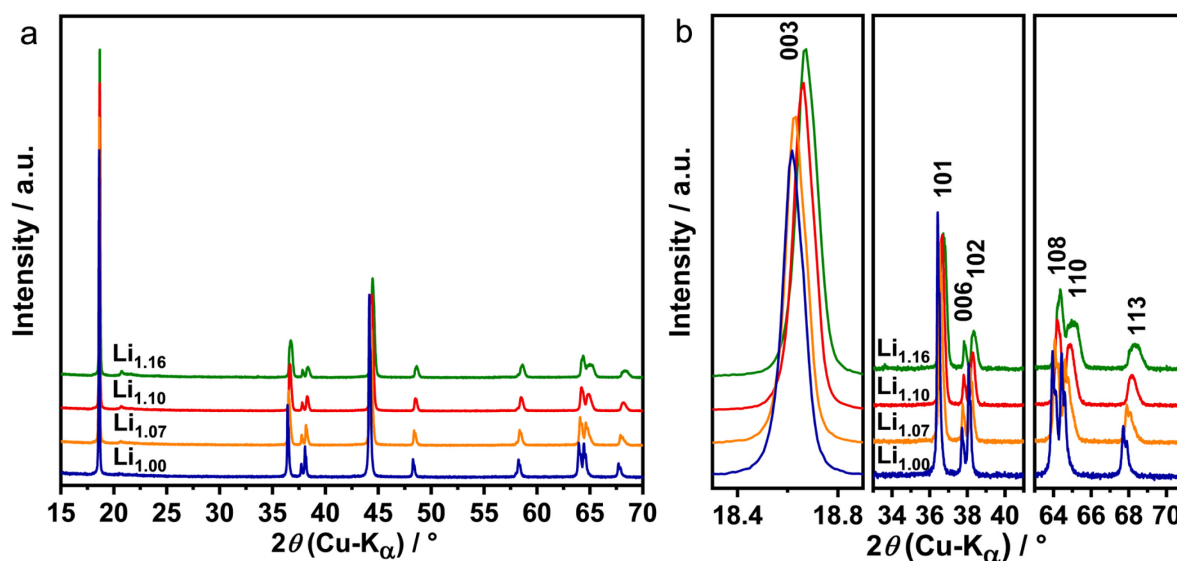
Figure S2. XRD pattern of $Li_{1.00}$ (blue), $Li_{1.07}$ (orange), $Li_{1.10}$ (red) and $Li_{1.16}$ (green): a) overview and b) details of selected reflections.

Table S1. Calculated Rietveld refinement parameters based on the structural model for $LiMn_{0.5}Ni_{0.5}O_2$ of Bréger et al.[1]: space group, lattice parameters, Cell Volume V, cation occupancies, atom coordinate z of the oxide ions, the estimated crystallite size (integral breadth) and the R factor.

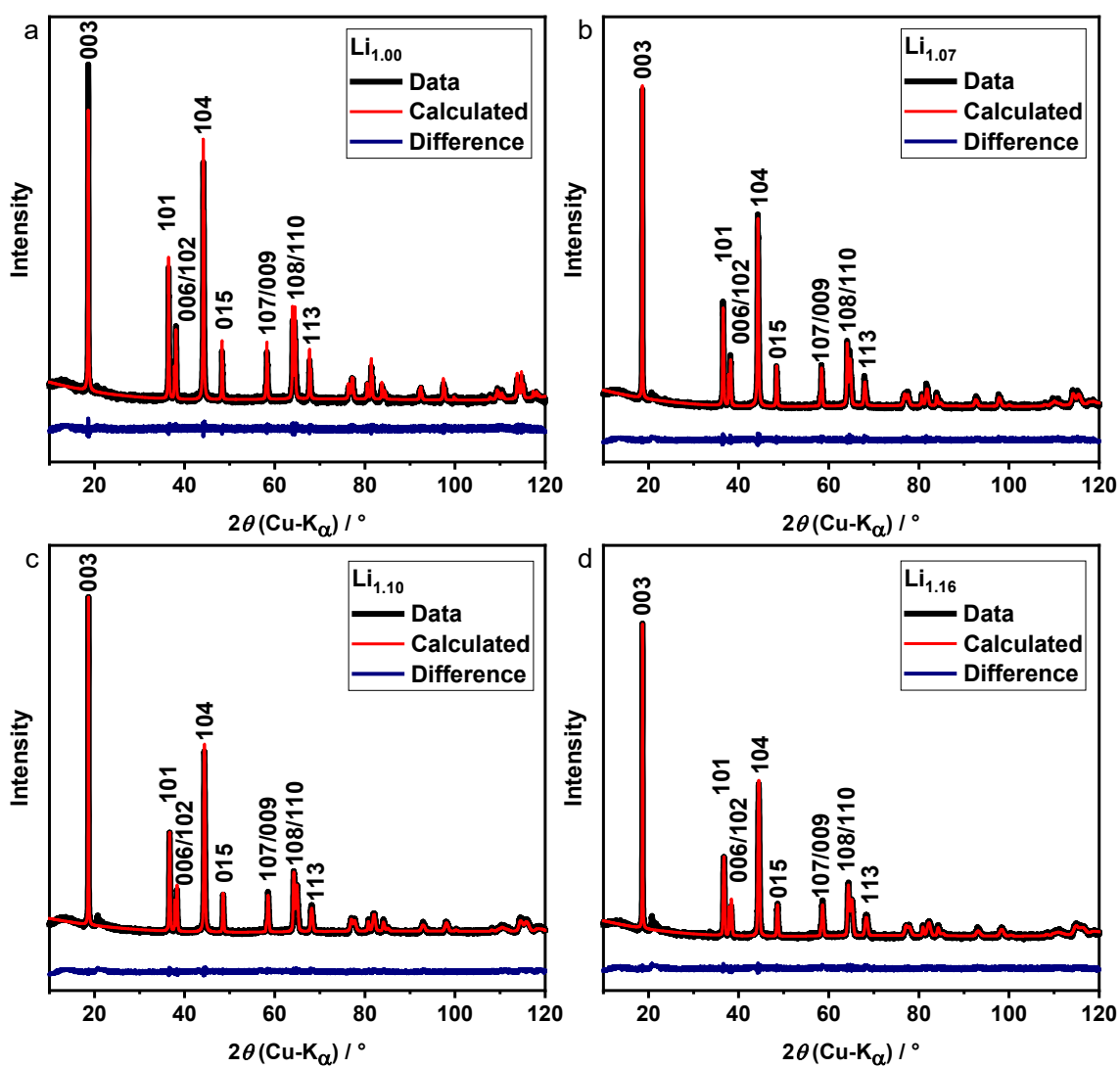|	$Li_{1.00}$	$Li_{1.07}$	$Li_{1.10}$	$Li_{1.16}$
Space group	$R\bar{3}m$ (166)	$R\bar{3}m$ (166)	$R\bar{3}m$ (166)	$R\bar{3}m$ (166)
***a* / Å**	2.890	2.880	2.874	2.867
***c* / Å**	14.306	14.289	14.272	14.255
V / Å³	103.5	102.6	102.1	101.5
Li_{Li} (3a: 0, 0, 0)	0.91	0.92	0.93	0.94
Ni_{Li} (3a: 0, 0, 0)	0.09	0.08	0.07	0.06
Li_{TM} (3b: 0, 0, 1/2)	0.09	0.08	0.07	0.06
Mn_{TM} (3b: 0, 0, 1/2)	0.50	0.50	0.50	0.50
Ni_{TM} (3b: 0, 0, 1/2)	0.41	0.42	0.43	0.44
z [O (6c: 0, 0, z)]	0.242	0.243	0.243	0.243
Crystallite Size / nm	149	385	284	293
R_{wp} / %	5.8	5.9	4.6	5.3

Figure S3. XRD pattern (black) of a) $Li_{1.00}$, b) $Li_{1.07}$, c) $Li_{1.10}$ and d) $Li_{1.16}$ in comparison with the calculated pattern from Rietveld refinement (red) and the difference between both (blue).
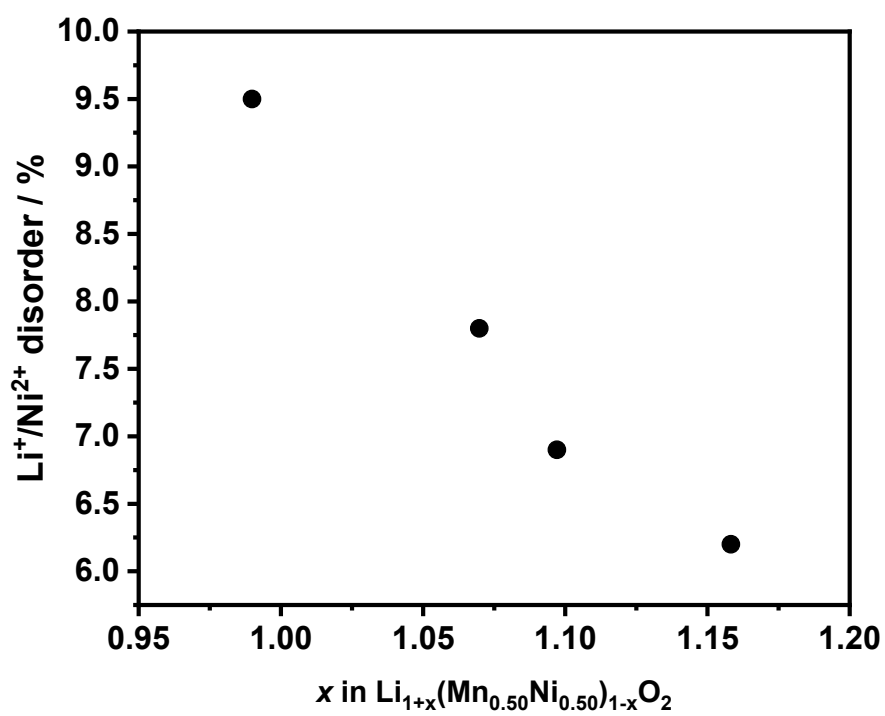
Figure S4. Li/Ni disorder as a function of the amount of excess Li^+ in the structure determined via Rietveld refinement.
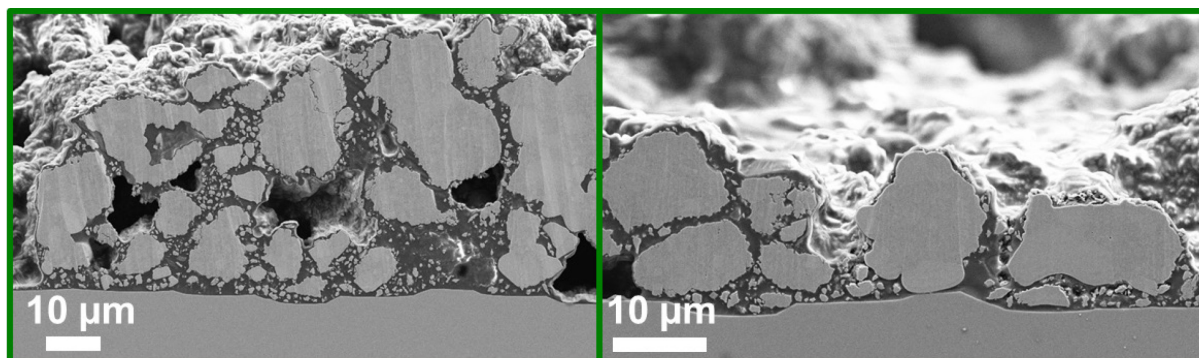

Figure S5. Overview SEM images of $Li_{1.16}$ particle cross section showing an irregular morphology and the local phase separation.
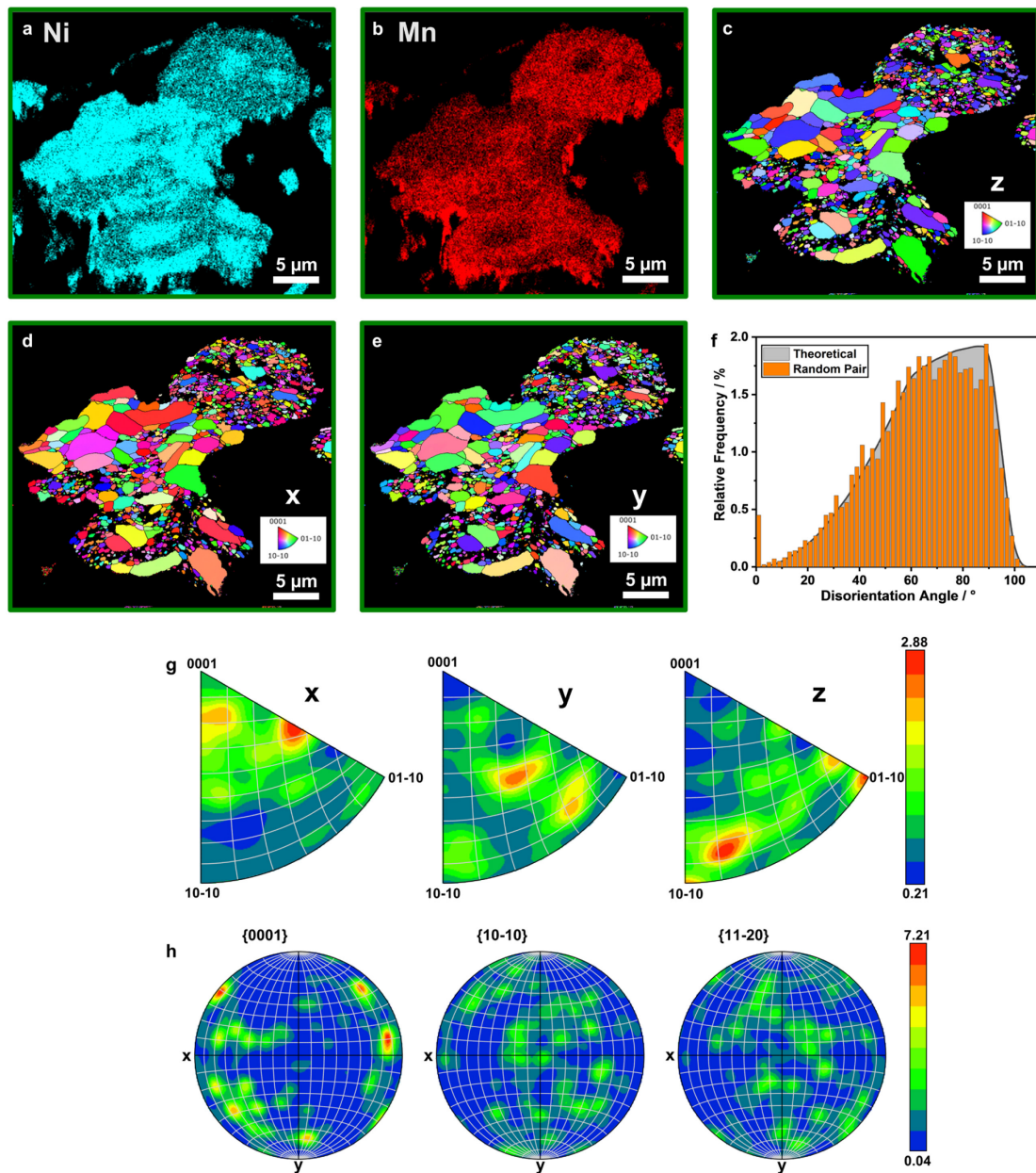
Figure S6. EBSD results of $Li_{1.16}$: EDX mapping of a) Ni and b) Mn, orientation distribution maps with inverse pole figure color key in direction c) Z, d) X and e) Y with respect to the acquisition system. The specimen is located in the X-Y plane and is oriented perpendicularly to the Z-axis. Furthermore, g) the inverse pole figures for the three directions X, Y and Z and h) pol figures for the families {0001}, {10-10} and {11-20} indicating both no significant preferred crystallographic orientation of the crystallites. This is confirmed by f) the correlation of the Mackenzie plot (grey) with the random pair distribution (orange) of 99 % and an M-index of 0.1, where a M-index of 1 represents a single crystal and a value of 0 represents a purely random orientation distribution.[2]
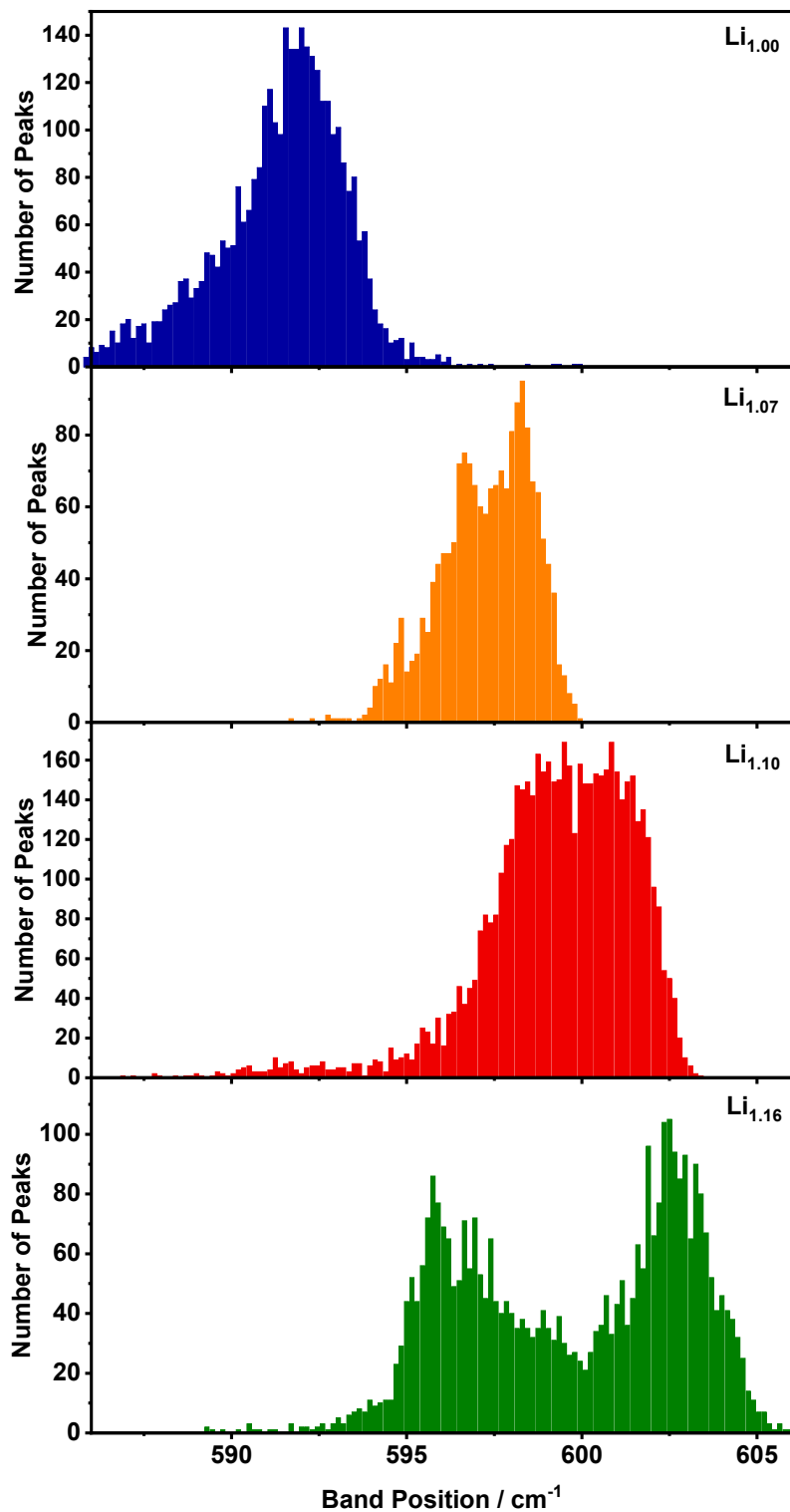
Figure S7. Histograms of the fitted position of the Raman vibration band at approximately 600 cm^{-1} of Li$_{1.00}$ (blue), Li$_{1.07}$ (orange), Li$_{1.10}$ (red) and Li$_{1.07}$ (green).
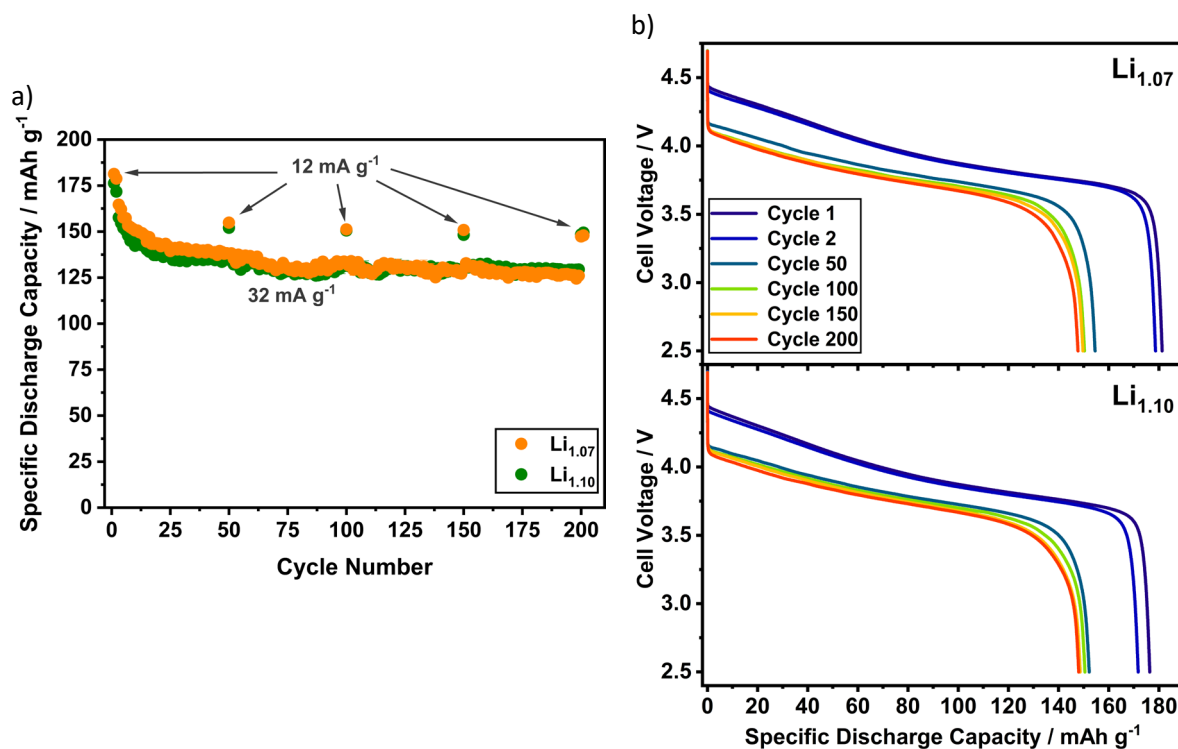
Figure S8. Long-term cycling performance of $Li_{1.07}$ and $Li_{1.10}$ at RT (2.5 - 4.7 V): a) Specific discharge capacities and b) discharge voltage profiles of cycles with lower discharge current (12 mA g^{-1}). The small fluctuation of the data points in a) is related to slight variations of the room temperature.
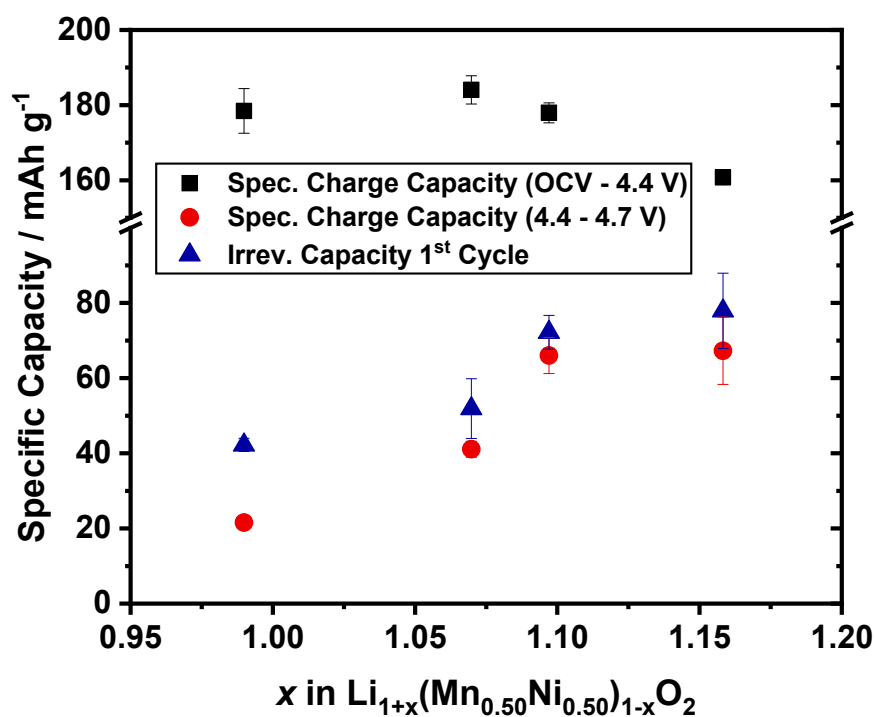

Figure S9. Electrochemical analysis of the 1st cycle specific capacity behavior in different voltage ranges: OCV – 4.4 V (black) and 4.4 – 4.7 V (red) as well as the irreversible initial capacity loss. The given numbers are mean values of three cells.
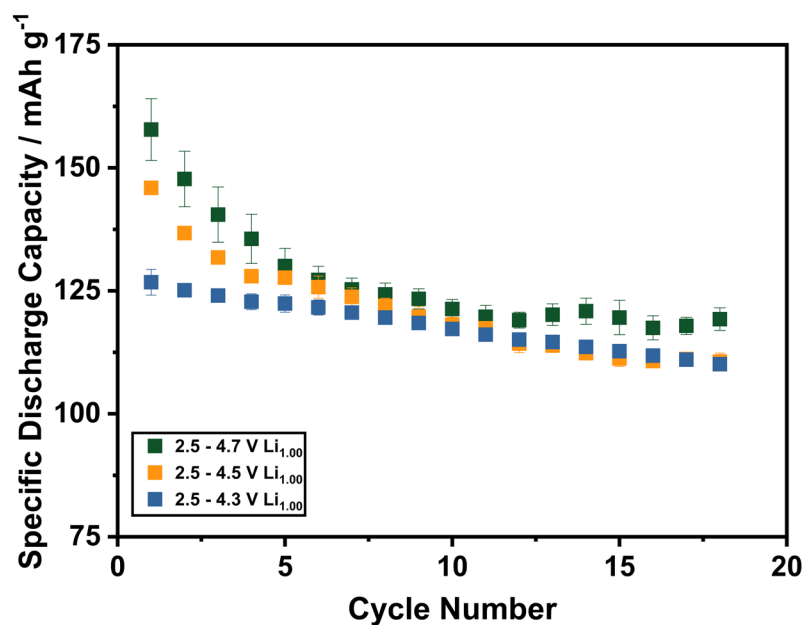
Figure S10. Comparison of the discharge capacity development during cycling (12 mA g^{-1}) of Li$_{1.00}$ using different upper cut-off voltages: 4.3 V (blue), 4.5 V (yellow) and 4.7 V (green).
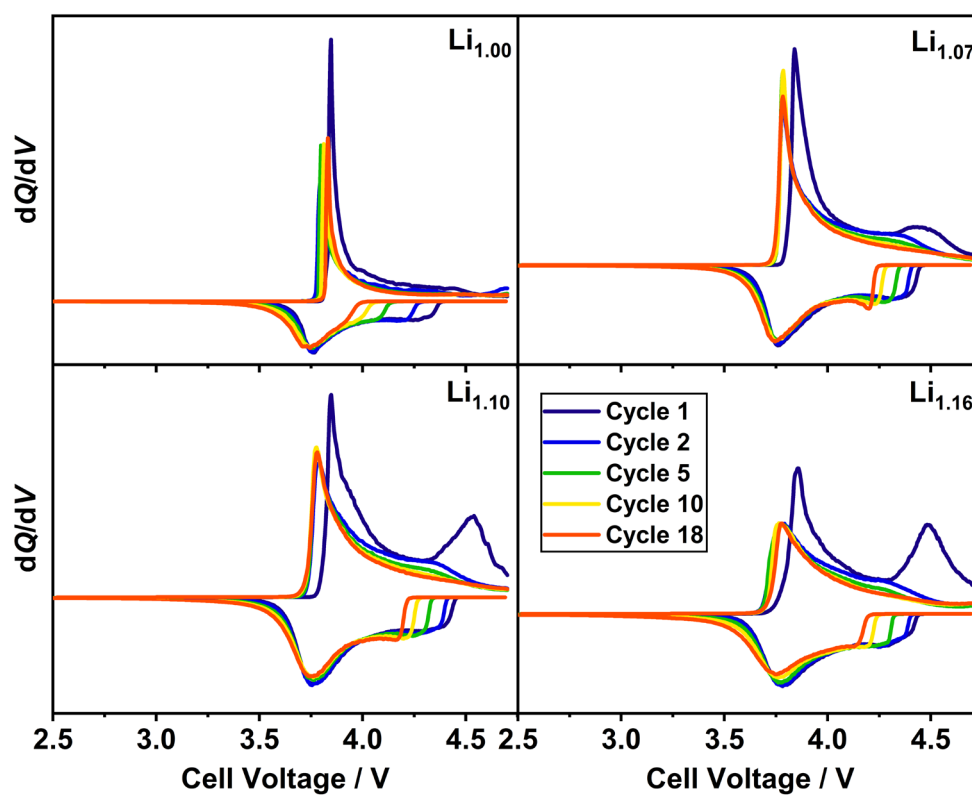

Figure S11. Electrochemical characterization of Li$_{1.00}$, Li$_{1.07}$, Li$_{1.10}$ and Li$_{1.16}$ during the initial cycles (12 mA g^{-1}): supplementary dQ/dV plots of the cycling data presented in Figure 9.

References

1   J. Bréger, Y. S. Meng, Y. Hinuma, S. Kumar, K. Kang, Y. Shao-Horn, G. Ceder and C. P. Grey, *Chem. Mater.*, 2006, **18**, 4768.

2   P. Skemer, I. Katayama, Z. Jiang and S. Karato, *Tectonophysics*, 2005, **411**, 157.